blood®
Regular Article

HEMATOPOIESIS AND STEM CELLS

Loss of endothelial membrane KIT ligand affects systemic KIT ligand levels but not bone marrow hematopoietic stem cells

Sahoko Matsuoka,[1,*] Raffaella Facchini,[1,*] Tiago C. Luis,[1,2,*] Joana Carrelha,[1,*] Petter S. Woll,[3,*] Takuo Mizukami,[1] Bishan Wu,[1] Hanane Boukarabila,[1] Mario Buono,[4] Ruggiero Norfo,[1] Fumio Arai,[5] Toshio Suda,[6] Adam J. Mead,[1,4] Claus Nerlov,[4,†] and Sten Eirik W. Jacobsen[1,3,4,7,8,†]

[1]Haematopoietic Stem Cell Biology Laboratory, Medical Research Council Molecular Haematology Unit, Medical Research Council Weatherall Institute of Molecular Medicine, University of Oxford, Oxford, United Kingdom; [2]Department of Immunology and Inflammation, Centre for Inflammatory Disease, Imperial College London, London, United Kingdom; [3]Department of Medicine Huddinge, Center for Hematology and Regenerative Medicine, Karolinska Institutet, Stockholm, Sweden; [4]Medical Research Council Molecular Haematology Unit, Medical Research Council Weatherall Institute of Molecular Medicine, University of Oxford, Oxford, United Kingdom; [5]Department of Stem Cell Biology and Medicine, Graduate School of Medical Sciences, Kyushu University, Fukuoka, Japan; [6]Cancer Science Institute, National University of Singapore, Singapore, Singapore; [7]Department of Cell and Molecular Biology, Karolinska Institutet, Stockholm, Sweden; and [8]Karolinska University Hospital Huddinge, Stockholm, Sweden

KEY POINTS

- **Endothelial KIT ligand deletion reduces systemic KIT ligand, precluding conclusions on role of endothelial niche expression of KIT ligand.**
- **HSC homeostasis is regulated primarily by soluble rather than membrane KIT ligand expression in endothelial cells.**

A critical regulatory role of hematopoietic stem cell (HSC) vascular niches in the bone marrow has been implicated to occur through endothelial niche cell expression of KIT ligand. However, endothelial-derived KIT ligand is expressed in both a soluble and membrane-bound form and not unique to bone marrow niches, and it is also systemically distributed through the circulatory system. Here, we confirm that upon deletion of both the soluble and membrane-bound forms of endothelial-derived KIT ligand, HSCs are reduced in mouse bone marrow. However, the deletion of endothelial-derived KIT ligand was also accompanied by reduced soluble KIT ligand levels in the blood, precluding any conclusion as to whether the reduction in HSC numbers reflects reduced endothelial expression of KIT ligand within HSC niches, elsewhere in the bone marrow, and/or systemic soluble KIT ligand produced by endothelial cells outside of the bone marrow. Notably, endothelial deletion, specifically of the membrane-bound form of KIT ligand, also reduced systemic levels of soluble KIT ligand, although with no effect on stem cell numbers, implicating an HSC regulatory role primarily of soluble rather than membrane KIT ligand expression in endothelial cells. In support of a role of systemic rather than local niche expression of soluble KIT ligand, HSCs were unaffected in KIT ligand deleted bones implanted into mice with normal systemic levels of soluble KIT ligand. Our findings highlight the need for more specific tools to unravel niche-specific roles of regulatory cues expressed in hematopoietic niche cells in the bone marrow.

Introduction

Hematopoietic stem cells (HSCs), safeguarding life-long replenishment of all blood cell lineages, are tightly controlled by intrinsic and extrinsic cues.[1] The concept that extrinsic HSC regulation is largely achieved locally within distinct HSC niches was proposed more than 4 decades ago.[2] Developments facilitating identification, imaging, and cellular and molecular characterization of HSCs and their neighboring candidate niche cells have provided evidence of anatomical HSC niches in the bone marrow (BM).[3-5] Although controversy remains regarding the exact cell types that constitute HSC niches,[3-12] candidate HSC niches are vascularized[3-5] and include endothelial cells (ECs).[7] However, evidence for anatomical HSC niches does not in itself address whether the proposed niche cells have critical HSC-sustaining roles. Genetic experiments have been conducted to address this, including ablation of candidate niche cell types in the BM, resulting in phenotypes compatible with an HSC niche regulatory role for a number of cell types.[6,8-11] However, this interpretation has been disputed[3-5] because the observed HSC phenotypes may reflect systemic rather than niche cell-specific roles of ablated cell types and the soluble extrinsic regulators they produce, because the targeted cell types are not restricted to the BM or proposed HSC niches. Therefore, knocking out key regulatory molecules expressed in candidate BM HSC niche cells has been used as an alternative and potentially more specific approach to establish the direct regulatory roles of HSC niche cells.

KIT ligand (*Kitl*, also known as stem cell factor or steel factor) and its receptor KIT were initially discovered through the shared pleiotropic effects of germ line mutations in the Steel (*Sl*) and dominant-white spotting (*W*) locus, respectively, resulting in deficiencies in gametogenesis, melanogenesis, and hematopoiesis of different severity dependent on the type of mutation.[13] In mice homozygous for the *Sl* mutation, resulting in the deletion of the *Kitl* coding sequences, a complete loss of KITL expression is observed, resulting in lethality late in gestation.[14] Within the BM, where KITL is known to play a key role in the regulation of HSC numbers,[1,3-5] ECs and leptin receptor positive perivascular stromal cells (LEPR^{+} PVCs) express the highest levels of *Kitl*.[15] The identification of the membrane-bound expression of KITL (mKITL),[16] which when membrane bound would probably require direct cell-cell contact between HSCs that express the receptor KIT and the BM niche cells that express mKITL, including ECs and PVCs,[7,17] and the finding that Steel-Dickie (*Sld*) mutant mice that express only soluble KITL (sKITL) have a severe HSC defect,[5,18,19] have been interpreted as evidence that mKITL acts locally in creating a BM HSC niche.[5,7,20] Combined with the conditional deletion of *Kitl* (required for sKITL and mKITL expression) in ECs, resulting in reduced HSC numbers in the BM of adolescent as well as adult mice,[7] this was interpreted as evidence for a perivascular HSC niche in the BM in which EC-derived mKITL regulates HSC maintenance.[5] However, more recently we also demonstrated that circulating sKITL is drastically reduced in *Sld* mutant mice.[21] Heterozygous germ line *Kitl* knockout mice display a reduction in HSC numbers[7] and a corresponding gene dosage effect on the systemic sKITL levels.[21] Because KITL is expressed by ECs outside and throughout the BM,[22-24] this raised the alternative possibility that EC-derived KITL might sustain HSCs primarily through sKITL, potentially produced outside the HSC niche or even outside the BM, rather than through the proposed endothelial niche cell expression of mKITL.[5,7] Herein, we pursued experiments to provide further insights into the regulatory roles of EC-derived systemic sKITL and EC niche–presented mKITL.

Methods

Mouse lines

Genetically modified mouse models used in the study are summarized in supplemental Table 1, available on the *Blood* website. Mice allowing for the conditional deletion of *Kitl* (Kitl$^{tm2.1Sjm}$/J; Δ), encoding sKITL and mKITL, and *Kitl*$^{LEx7/LEx7}$ (LEx7) mice allowing for the conditional deletion of mKITL have been described.[7,21] LEx7 mice had been backcrossed onto a C57BL/6 background for >5 generations. *Kitl*$^{\Delta Ex7/\Delta Ex7}$ (ΔEx7) mice, with germ line deletion of *mKitl*, were generated by crossing LEx7 mice with *CMV-Cre*$^{tg/+}$ (B6.C-Tg[CMV-cre]1Cgn/J) mice.[25] Conditional cell-specific deletion of *mKitl* was induced by crossing LEx7 mice with *Tie2-Cre*$^{tg/+}$ (B6.Cg-Tg[Tek-cre]1Ywa/J) mice (The Jackson Laboratory, stock 008863), *LepR*$^{Cre/+}$ (B6.129[Cg]-Lepr$^{tm2(cre)Rck}$/J) mice,[7,26] or *Amh-Cre*$^{tg/+}$ (B6.FVB[129S]-Tg(Amh-cre)8815Reb/J) mice.[27] *LepR*$^{Cre/+}$ mice were identical to those previously used to study the role of KITL in hematopoiesis.[7,28] The genotyping strategy used to distinguish *Tie2-Cre*^{tg} and *LepR*^{Cre} alleles (supplemental Figure 1) was identical to that in previous studies.[7]

Kitl-tdTomato$^{tg/+}$ mice have been described,[21] and *Sl/+* (WC/ReJ Kitl^{Sl}/J) mice[29] were from The Jackson Laboratory (stock 000693). LEx7 mice,[21] *Sl/+* mice,[30] and *LepR*$^{Cre/+}$ mice[7] were genotyped as previously described, whereas primers for genotyping ΔEx7, *CMV-Cre*$^{tg/+}$, *Amh-Cre*$^{tg/+}$, and *Tie2-Cre*$^{tg/+}$ mice are specified as follows: ΔEx7 forward primer 5′-CTTGCCTCGAGCCCTTAAT-3′ and ΔEx7 reverse primer 5′-GCCCTTAAGTGTGCCTTGTC-3′ (ΔEx7 <200 bp); *CMV-Cre*$^{tg/+}$ and *Amh-Cre*$^{tg/+}$ forward primer 5′-CGTTTTCTGAGCATACCTGGA-3′ and *CMV-Cre*$^{tg/+}$ and *Amh-Cre*$^{tg/+}$ reverse primer 5′-ATTCTCCCACCGTCAGTACG-3′ (Tg: 450 bp); *Tie2-Cre*$^{tg/+}$ forward primer 5′-CCTGTGCTCAGA-CAGAAATG-3′ and *Tie2-Cre*$^{tg/+}$ reverse primer 5′-GGCAAA TTTTGGTGTACGGTC-3′ (Tg: ~200 bp); and *Kitl-tdTomato*$^{tg/+}$ forward$_{Tomato}$ primer 5′-CACCTCCCACAACGAGGACTACACC-3′, *Kitl-tdTomato*$^{tg/+}$ forward$_{Kitl\text{-}UTR}$ primer 5′-GGGCTTCATTTGCT GTCTGTCACC-3′, and *Kitl-tdTomato*$^{tg/+}$ reverse$_{Kitl}$ primer 5′-TCTCACACCACGCCTGTCTCTCC-3′ (wild-type: 331 bp; *Kitl-tdTomato*$^{tg/+}$: 588 bp).

All mice were maintained at the Biomedical Services animal facility, University of Oxford, in accordance with the United Kingdom Home Office regulations, and the procedures were performed under ethical license number 30/3103, approved by the Oxford University Clinical Medicine Ethical Review Committee.

Flow cytometry

Bones were processed by crushing in a mortar before counting the cellularity with a Sysmex cell counter. Mouse BM and spleen HSCs and myeloid progenitors and peripheral blood (PB) cell lineages were analyzed as described.[31,32] Antibodies (supplemental Table 2) were titrated and specificity controlled based on simultaneous analysis of cell populations lacking expression of the antigens and/or by using isotype control antibodies from the same companies as those of specific antibodies. Dead cells were excluded using 7-amino-actinomycin D or 4′,6-diamidino-2-phenylindole (DAPI). Stained cells were acquired on a BD LSRII or a BD LSRFortessa X-20 (BD Biosciences) and analyzed using FlowJo analysis software (TreeStar Inc).

Enzyme-linked immunosorbent assay

Mouse PB serum samples were clotted for 2 hours and centrifuged for 20 minutes at 2000*g*. Bone extracellular fluid samples were collected, as previously described,[33] from 1 mouse femur by removing distal epiphysis, followed by 1 minute centrifugation at 3000*g*, allowing for collection of BM fluid into 1.5 mL Eppendorf tubes containing 50 μL phosphate-buffered saline. Collected cells were mixed by pipetting and centrifuged for 3 minutes at 300*g*, followed by the collection of supernatant. Isolated serum and BM fluid were assessed by KITL enzyme-linked immunosorbent assay kit (R&D systems), as described.[21] Optical density was measured on microplate reader (Molecular Devices-SpectraMaxM2e) set to 450 nm, with a wavelength correction of 570 nm. Concentration was extrapolated from a standard curve run for each individual experiment.

Quantitative reverse transcription PCR

Two thousand cells were fluorescence-activated cell sorted directly into Trizol Reagent (Invitrogen), and RNA was isolated. Reverse transcription was performed using Superscript Vilo complementary DNA synthesis kit (Invitrogen). Quantitative polymerase chain reaction (qPCR) was performed with Taqman Gene Expression Assays (Applied Biosystems): total *Kitl*, Mm00442972_m1; m*Kitl*, Mm01232339_m1; and *Hprt*, Mm01545399_m1. Data were analyzed with ΔCt method, using housekeeping gene *Hprt*, or mean of housekeeping genes *B2m*,

Gapdh, and *Hprt*, for normalization. Alternatively, 50 cells were sorted directly into CellsDirect 2X reaction mix with Taqman Gene Expression Assays. Samples were subjected to targeted complementary DNA amplification for 22 cycles, diluted 1:5 in Tris-EDTA buffer before multiplex qPCR analysis using the Biomark 96.96 Dynamic Array platform.[34]

Competitive BM transplantation

Functional assessment of HSC activity was performed through competitive long-term BM reconstitution experiments,[31] the gold standard for assessing HSC activity.[35] BM mononuclear cells (2×10^6) from CD45.2 donor mice were intravenously transplanted with unfractionated support/competitor CD45.1 BM cells (2×10^6) into lethally irradiated (split dosage of 500 cGy each) C57BL/6 (CD45.1) recipient mice (>8 weeks old). Flow cytometry analysis of CD45.1 and CD45.2 contribution to mature PB lineages and BM HSCs was performed 16 weeks after transplantation.[31] For competitive transplantations with cells from femurs implanted under the kidney capsule, 5×10^6 donor cells (CD45.2) were transplanted together with 2.5×10^5 support BM CD45.1 cells into CD45.1 recipients.

Renal subcapsular bone transplantation assay

Wild-type, *Kitl-tdTomato*$^{tg/+}$, and *Sl/Sl* embryos, on a CD45.2 background, were collected from pregnant mice at embryo day (E) 15.5, and femurs dissected under stereomicroscope. Both femurs from each embryo were surgically transplanted under the kidney capsule of 8- to 14-week-old wild-type mice with normal serum KITL levels, under anesthesia.[36,37] CD45.1 recipients were used for evaluation of hematopoietic chimerism in transplanted bones, and CD45.2 recipients were used for evaluating HSC activity within kidney capsule–transplanted bones. Grafted bones were dissected from the kidney 3 to 4 weeks after transplantation, and the BM analyzed for cellularity, HSC and progenitor numbers, and long-term competitive repopulating ability.

Immunohistochemistry

Dissected testicles were cryo-embedded and sectioned (8-10 μm). Sections were fixed with methanol, blocked with protein (Dako), and incubated overnight at 4°C with primary antibodies. Stained sections were incubated with secondary antibodies for 2 hours and mounted with coverslips using ProLong Gold Antifade Reagent (Invitrogen). Antibodies used are shown in supplemental Table 2. Immunofluorescence data were acquired with a BioRad Radiance 2000 laser scanning confocal microscope or Olympus FV1000 confocal microscope. Images were analyzed using Fiji/ImageJ software with manual identification of spermatogonial precursor cells (SPCs) and KIT$^+$ cells.

Statistical analysis

Unless otherwise specified, data sets were analyzed using the nonparametric Mann-Whitney test to assess statistical significance.

Results

Endothelial KITL deletion results in reduced systemic KITL levels and HSC numbers

Using the same *Tie2-Cre*^{tg} (B6.Cg-Tg[Tek-cre]1Ywa/J) conditional targeting as in previous studies[7] to delete the floxed *Kitl* (Kitl$^{tm2.1Sjm}$/J; Δ) allele (encoding mKITL and sKITL) in ECs of heterozygous *Sl* (WC/ReJ Kitl^{Sl}/J) mice (*Sl*/Tie2Δ), we observed, as previously reported,[7] a significant reduction (35%) in BM HSCs in *Sl*/Tie2Δ mice aged 4 weeks, as assessed by flow cytometry (Figure 1A-C), which was confirmed by a significant reduction in HSC long-term repopulating activity, as assessed by competitive transplantation (Figure 1D; supplemental Figure 2A-B). *Sl*/Tie2Δ mice also had a significant reduction in committed erythroid progenitor cells (Figure 1E; supplemental Figure 2C). However, and to our knowledge, not previously investigated, this was also accompanied by significantly reduced (39%) systemic levels of sKITL (Figure 1F; supplemental Table 3). Combined with the fact that KITL is produced by ECs in multiple other tissues and organs,[22,23,38] this precludes the conclusion that maintenance of HSCs in BM is dependent on KITL produced by ECs within HSC niches[5] or even ECs in the BM.

mKITL expressed by ECs is not critical for HSC maintenance in BM

We recently generated a novel mouse model allowing for the selective conditional depletion of mKITL.[21] Here, we used this model to study the role of mKITL in steady-state HSC maintenance, because mKITL has been proposed to play an important local role in the regulation of HSCs in BM.[5,18-20] Mice with germ line homozygous deletion of *Kitl* exon 7 (*Kitl*$^{\Delta Ex7/\Delta Ex7}$; ΔEx7), encoding the transmembrane domain required for membrane localization of mKITL, were born at a reduced Mendelian ratio and with a white coat color (supplemental Figure 3A-B), characteristic of KITL deficiency. The BM of ΔEx7 mice had significantly reduced cellularity ($P < .01$) and 50%-reduced HSC numbers, although not reaching statistical significance ($P = .06$; Figure 1G-H; supplemental Figure 3C). Germ line deletion of mKITL also resulted in a reduction of several committed myeloerythroid progenitor cells (Figure 1I). However, in addition to a complete loss of mKITL, we previously demonstrated a >60% reduction in systemic sKITL in ΔEx7 mice aged 3 weeks and also that circulating sKITL is drastically reduced in *Sld* mutant mice (supplemental Table 3),[21] precluding any conclusion about the observed hematopoietic defects reflecting a niche or local role of mKITL in the BM.

In 4- to 6-week-old adolescent *Tie2-Cre*$^{tg/+}$;*Kitl*$^{LEx7/LEx7}$ (Tie2ΔEx7) mice, in which mKITL expression was specifically and efficiently deleted from ECs (Figure 2A; supplemental Figure 1), we also observed a significant (26%) reduction in circulating sKITL levels (Figure 2B; supplemental Table 3) but without any concomitant reduction of BM sKITL (Figure 2C; supplemental Table 4) and BM cellularity (Figure 2D), myeloerythroid progenitor cells (Figure 2E), or phenotypically and functionally defined HSCs (Figure 2F-H; supplemental Figure 4).

Although *LepR*^{Cre}-induced recombination in LEPR$^+$ PVCs has been shown to be very inefficient in young mice,[15] *LepR*^{Cre}-induced targeting of a floxed *Kitl* allele (encoding mKITL and sKITL) was reported to result in significant reductions in HSCs in the BM of 1-month-old mice; however, *Kitl* expression was not investigated in targeted LEPR$^+$ PVCs.[7] In light of this, we investigated the impact of combined targeting of floxed *mKitl* alleles in ECs and LEPR$^+$ PVCs on HSCs in the BM of 4- to 6-week-old mice

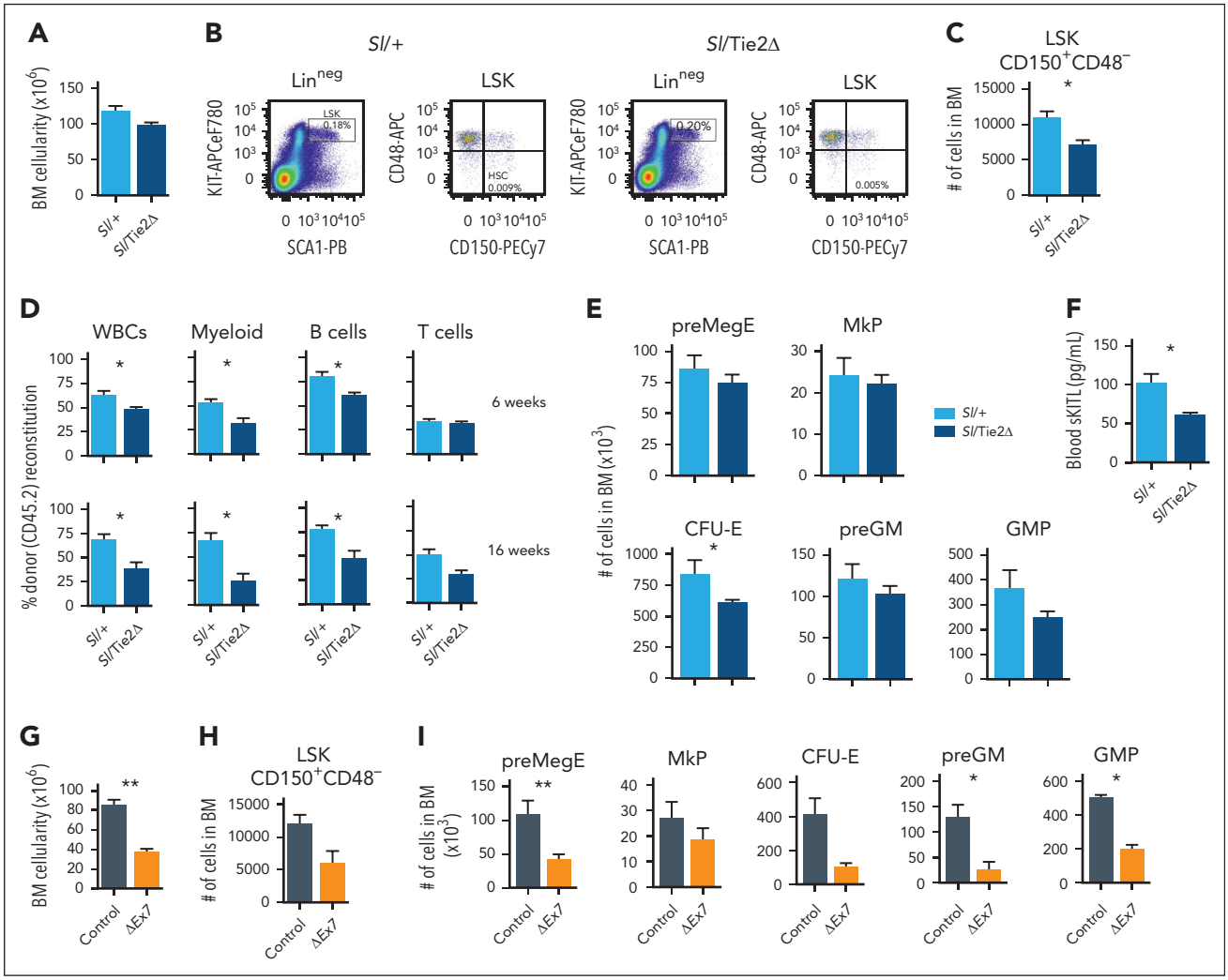

Figure 1. Endothelial *Kitl* deletion results in reduced HSC numbers and reduced systemic levels of sKITL. (A) Mean (± standard error of mean [SEM]) total BM mononuclear cells from 2 femurs and 2 tibias of 4-week-old *Sl*/+ (n = 3) and *Sl*/Tie2Δ (n = 5) mice. (B-C) Representative fluorescence-activated cell sorter (FACS) profiles with gated cell populations as percentages of total BM cells (B) and mean (± SEM) Lineage$^-$Sca1$^+$KIT$^+$ (LSK) CD150$^+$CD48$^-$ HSC numbers (C) of 4-week-old *Sl*/+ (n = 3) and *Sl*/Tie2Δ (n = 5) mice. (D) Mean (± SEM) percent donor (CD45.2) contribution in total PB toward total white blood cells (WBCs), MAC1$^+$GR1$^+$ myeloid cells, CD19$^+$ B cells, and CD4/CD8a$^+$ T cells 6 and 16 weeks after competitive transplantation of *Sl*/+ (n = 3 donors) or *Sl*/Tie2Δ (5 donors) BM cells. (E) Mean (± SEM) numbers of pre–megakaryocyte-erythroid (preMegE), megakaryocyte (MkP), colony forming unit–erythroid (CFU-E), pre–granulocute-monocyte (preGM), and granulocyte-monocyte (GMP) progenitor cells from 2 femurs and 2 tibias of 4-week-old *Sl*/+ (n = 3) and *Sl*/Tie2Δ (n = 5) mice. (F) Mean (± SEM) blood serum sKITL levels determined by enzyme-linked immunosorbent assay (ELISA) from 4-week-old *Sl*/+ (n = 4) and *Sl*/Tie2Δ (n = 5) mice. (G-H) Mean (± SEM) total BM mononuclear cell (G) and LSK CD150$^+$CD48$^-$ HSC (H) numbers from 2 femurs and 2 tibias of 3-week-old ΔEx7 and wild-type littermate controls (n = 5 per genotype). (I) Mean (± SEM) committed myelo-erythroid progenitor cell numbers from 2 femurs and 2 tibias of 3-week-old ΔEx7 and wild-type littermate controls (n = 4-5 per genotype). All data represent mean ± SEM, and the nonparametric Mann-Whitney test was used to assess statistical significance. *$P < .05$; **$P < .01$.

by crossing the same *LepR*$^{Cre/+}$ (B6.129(Cg)-Lepr$^{tm2(cre)Rck}$/J) mice used in previous studies[7] with Tie2ΔEx7 mice (supplemental Figure 1). Although *mKitl* expression was almost undetectable in ECs, no significant reduction in *mKitl* expression was observed in LEPR$^+$ PVCs purified from the BM of *Tie2-Cre*$^{tg/+}$;*Lep-R*^{Cre}*Kitl*$^{LEx7/LEx7}$ (Tie2,LepRΔEx7) mice (supplemental Figure 5A-B), and the blood and BM sKITL levels were not significantly different compared with those in Tie2ΔEx7 mice (supplemental Figure 5C-D; supplemental Tables 3 and 4). With the exception of erythroid progenitors that were reduced in Tie2,LepRΔEx7 but not Tie2-ΔEx7 mice, neither myeloid progenitors (supplemental Figure 5E-F) nor phenotypically or functionally defined HSCs were affected (supplemental Figures 4 and 5G-I). Furthermore, no significant differences in HSCs and multipotent progenitor populations were observed in the spleen from adolescent Tie2ΔEx7 or Tie2,-LepRΔEx7 mice (supplemental Figure 5J-L).

We next performed similar studies on adult (age, 13-15 weeks) Tie2ΔEx7 and Tie2,LepRΔEx7 mice, because adult mice have been shown to have a more pronounced reduction in HSCs upon conditional deletion of *Kitl* (encoding sKITL and mKITL) in ECs and PVCs.[7] Similar to adolescent mice, *mKitl* was almost undetectable in ECs from the BM of Tie2ΔEx7 and Tie2,-LepRΔEx7 mice (Figure 3A), and unlike in adolescent mice, a significant (59%) reduction was observed in *mKitl* expression in LEPR$^+$ PVCs from the BM of Tie2,LepRΔEx7 mice (Figure 3B). Moreover, a bigger drop in blood sKITL levels was observed in both Tie2ΔEx7 (40%) and Tie2,LepRΔEx7 (43%) mice than in

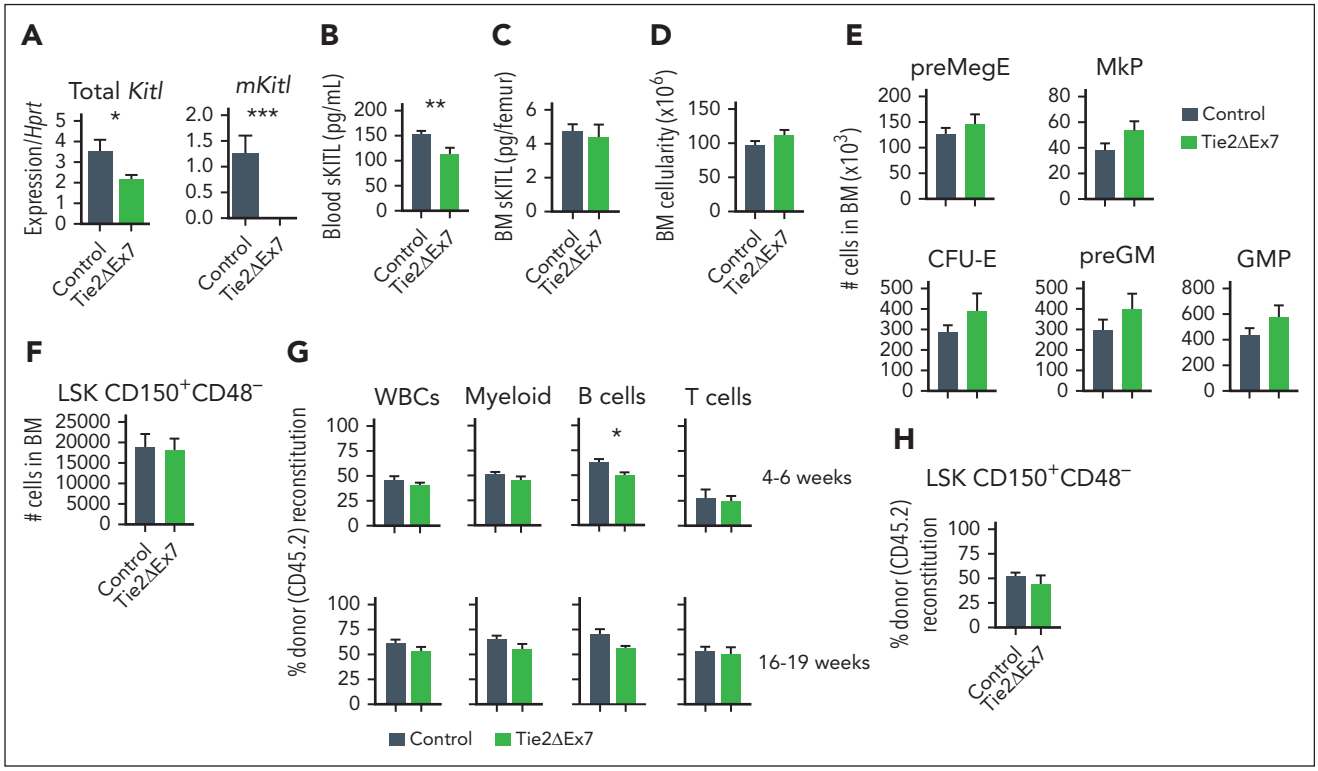

Figure 2. mKITL expressed by ECs is required for sustaining systemic sKITL levels but not BM HSCs in adolescent mice. (A) qPCR analysis of *Kitl* messenger RNA (mRNA) levels using *Kitl* exon 2-3–spanning (measuring total *Kitl* mRNA) and exon 7-8–spanning (measuring mRNA generating mKITL) amplicons on FACS-purified BM ECs ($CD45^-TER119^-CD31^+$) from 4- to 6-week-old Tie2ΔEx7 (n = 6) and wild-type littermate control mice (n = 13). Mean (± SEM) expression relative to *Hprt* is shown. (B) sKITL levels measured by ELISA in the blood serum from 4-week-old wild-type (control; n = 17) and Tie2ΔEx7 (n = 11) mice. The parametric Student *t* test was used for statistical analysis. (C) sKITL levels measured by ELISA in the BM extracellular fluid from 4-week-old wild-type (control; n = 10) and Tie2ΔEx7 (n = 4) mice. (D-F) Mean (± SEM) BM cellularity (D), number of committed myelo-erythroid progenitor cells (E) and LSK $CD150^+CD48^-$ HSCs (F) from 2 femurs and 2 tibias from 4- to 5-week-old wild-type (control; n = 11) and Tie2ΔEx7 (n = 9) mice. No significant ($P < .05$) differences detected by either a parametric or nonparametric *t* test. (G-H) Percent CD45.2 contribution to total WBCs, $MAC1^+GR1^+$ myeloid cells, $CD19^+$ B cells, and CD4/$CD8a^+$ T cells in the blood at 4 to 6 and 16 to 19 weeks (G), and BM LSK $CD150^+CD48^-$ HSCs at 16 to 19 weeks (H) after transplantation of BM from 5-week-old wild-type (control; n = 4) and Tie2ΔEx7 (n = 5) CD45.2 mice, in competition with wild-type CD45.1 BM cells. Unless otherwise specified, all data represent mean ± SEM, the nonparametric Mann-Whitney test was used to assess statistical significance. *$P < .05$; **$P < .01$; ***$P < .001$.

adolescent mice (Figure 3C; supplemental Table 3). Similar to young mice, sKITL levels were not reduced in the BM of Tie2-ΔEx7 and rather significantly increased in Tie2,LepRΔEx7 mice (Figure 3D; supplemental Table 4). However, similar to 4- to 6-week-old mice, no reduction in BM HSCs was observed (Figure 3E-F), and only megakaryocyte-erythroid progenitor cells among the myelo-erythroid progenitors were significantly reduced in both Tie2ΔEx7 and Tie2,LepRΔEx7 mice (Figure 3G). In agreement with previous studies of targeted deletion of both mKITL and sKITL,[7] a trend toward a higher number of spleen LSK $CD150^+CD48^-$ HSCs was observed in Tie2,LepRΔEx7 mice, whereas different multipotent progenitor cells were unaffected (supplemental Figure 6).

Locally produced KITL is critical for sustaining BM erythroid progenitors but not HSCs

We next sought to investigate whether deletion of *Kitl* exclusively in BM would result in an HSC phenotype. Because no *Cre* lines delete *Kitl* expression exclusively and efficiently in the whole BM, we instead used an assay in which long bones from *Sl/Sl* mice (completely lacking expression of sKITL and mKITL) or wild-type mice were implanted under the kidney capsule of wild-type mice with normal expression of mKITL and sKITL (supplemental Figure 7A).

Because *Sl/Sl* embryos die late in gestation,[13] we transplanted bones from E15.5 embryos. Previous studies implanting fetal *Sl/Sl* bones under the kidney capsule suggested that the number of LSK $CD150^+$ cells were not reduced,[36] but a more stringent, including functional, assessment of HSCs was not performed, and the prevalence of relevant niche cells and their expression of KITL was not investigated in the implanted bones. Hematopoiesis has been reported to not yet have colonized the BM at E15.5[39,40]. Therefore, this approach would also ensure that any observed hematopoietic phenotype would not reflect a pre-transplantation impact on HSCs because of the complete loss of KITL in all tissues of *Sl/Sl* embryos. However, because more recent studies suggested that rare HSCs reside in E15.5 fetal bones,[41] we first assessed to what degree transplanted bones from E15.5 embryos upon harvesting were populated by HSCs already present in the E15.5 bones or by HSCs from the recipient by transplanting bones from CD45.2 embryos into CD45.1 recipients. In agreement with previous studies,[36] analysis 3 weeks after bone transplantation revealed that all HSCs within both wild-type and *Sl/Sl* transplanted bones were from the recipient rather than transplanted bone (Figure 4A). Moreover, abundant ECs and $LEPR^+$ PVCs were sustained in both wild-type and *Sl/Sl* transplanted bones, although at variable frequencies (Figure 4B). Transplanted bones from *Kitl-tdTomato*

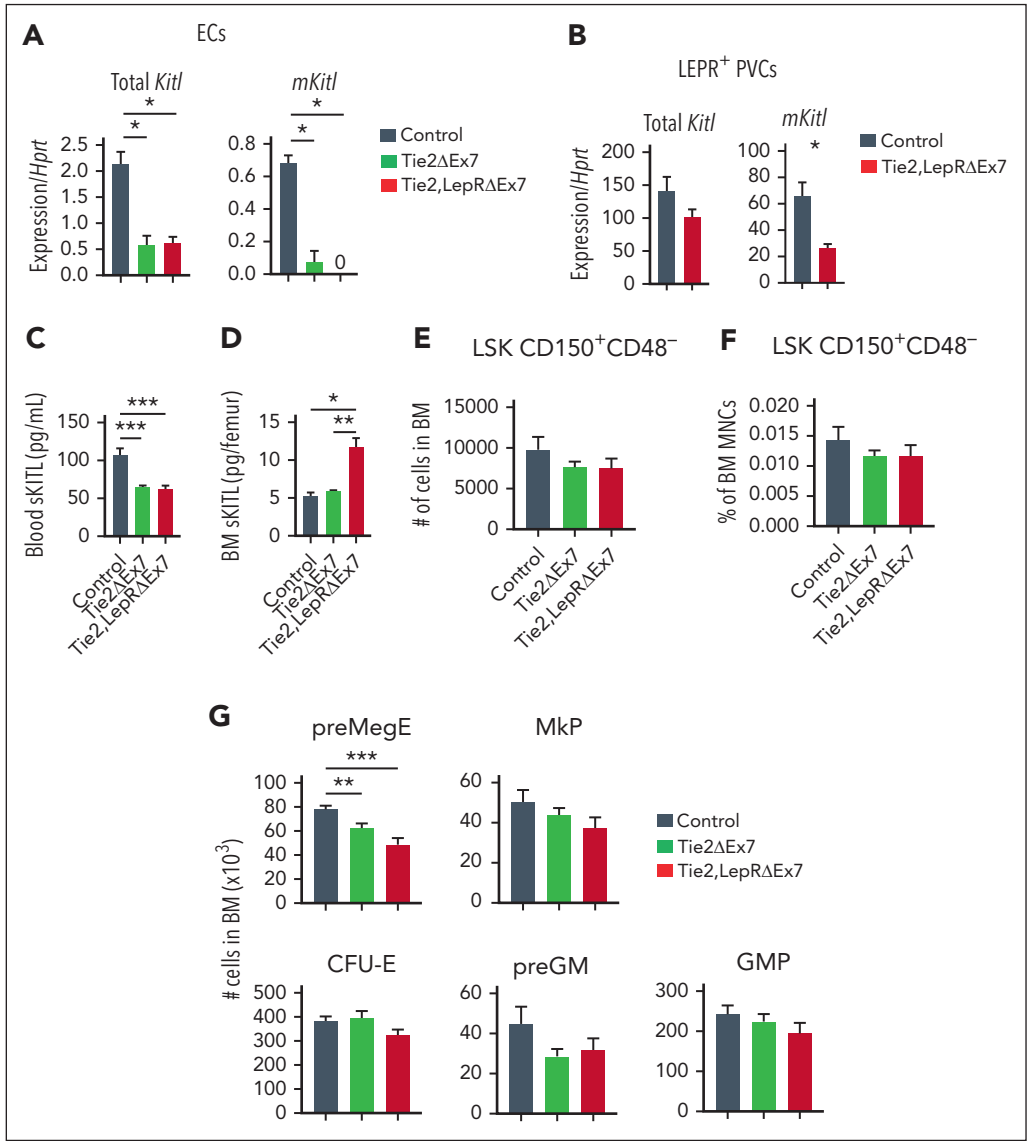

Figure 3. Endothelial expression of mKITL is required for sustaining normal levels of circulating sKITL but not BM HSCs in adult mice. (A-B) qPCR analysis of *Kitl* mRNA levels using *Kitl* exon 2-3–spanning (measuring total *Kitl* mRNA) and exon 7-8–spanning (measuring mRNA generating mKITL) amplicons in FACS-purified BM ECs (A) and LEPR$^+$ PVCs (CD45$^-$TER119$^-$CD31$^-$SCA1$^-$LEPR$^+$) (B) from 13- to 15-week-old Tie2ΔEx7 (n = 5), Tie2,LepRΔEx7 (n = 5-6) and wild-type littermate control (n = 3) mice. (C) sKITL levels measured by ELISA in the blood serum from 13- to 15-week-old wild-type (control, n = 10), Tie2ΔEx7 (n = 14) and Tie2,LepRΔEx7 (n = 14) mice. (D) sKITL levels measured by ELISA in the BM extracellular fluid from 13- to 15-week- old wild-type (control, n = 3), Tie2ΔEx7 (n = 5), and Tie2,LepRΔEx7 (n = 5) mice. (E-G) Mean (± SEM) number (E) and frequency (F) of LSK CD150$^+$CD48$^-$ HSCs, and number of committed myelo-erythroid progenitor cells (G) from 2 femurs and 2 tibias of 13- to 15-week-old wild-type (control; n = 7), Tie2ΔEx7 (n = 11), and Tie2,LepRΔEx7 (n = 8) mice. All data represent mean ± SEM, the nonparametric Mann-Whitney test was used to assess statistical significance. *$P < .05$; **$P < .01$; ***$P < .001$.

reporter mice[21] showed high and comparable tdTomato expression with nontransplanted bones in LEPR$^+$ PVCs, and in ECs, tdTomato expression was also sustained, although as expected,[15] at lower levels than in LEPR$^+$ PVCs (supplemental Figure 7B-C). In agreement with the *Kitl-tdTomato* data, LEPR$^+$ PVCs purified from transplanted wild-type bones expressed comparable levels of *Kitl* with that of non-transplanted bones and no detectable *Kitl* levels in LEPR$^+$ PVCs from transplanted *Sl/Sl* bones, demonstrating that LEPR$^+$ PVCs were entirely derived from transplanted bones (Figure 4C). In ECs isolated from transplanted *Sl/Sl* bones, *Kitl* was reduced by 76% compared with transplanted wild-type bones (Figure 4C), demonstrating that the majority of ECs originate from the transplanted bone but also some ECs derived from the recipient, probably reflecting vascularization of the transplanted bones.[36] Next, we phenotypically and functionally compared HSCs in transplanted bones from wild-type and *Sl/Sl* E15.5 embryos transplanted under the kidney capsule of wild-type mice (Figure 4D). No significant differences in BM HSCs were observed between transplanted wild-type and *Sl/Sl* bones, assessed phenotypically or functionally (Figure 4E-H). However, a large reduction in multiple stages of committed (Lin$^-$SCA1^{--}KIT$^+$) progenitors was observed (Figure 4I), including multiple established[32] stages of erythroid progenitors (Figure 4J-K), in agreement with the critical role of KITL in BM erythropoiesis.[42] Collectively, these results support that systemically provided sKITL regulates HSC numbers in the BM and fail to support a critical role of local BM production of either mKITL or sKITL.

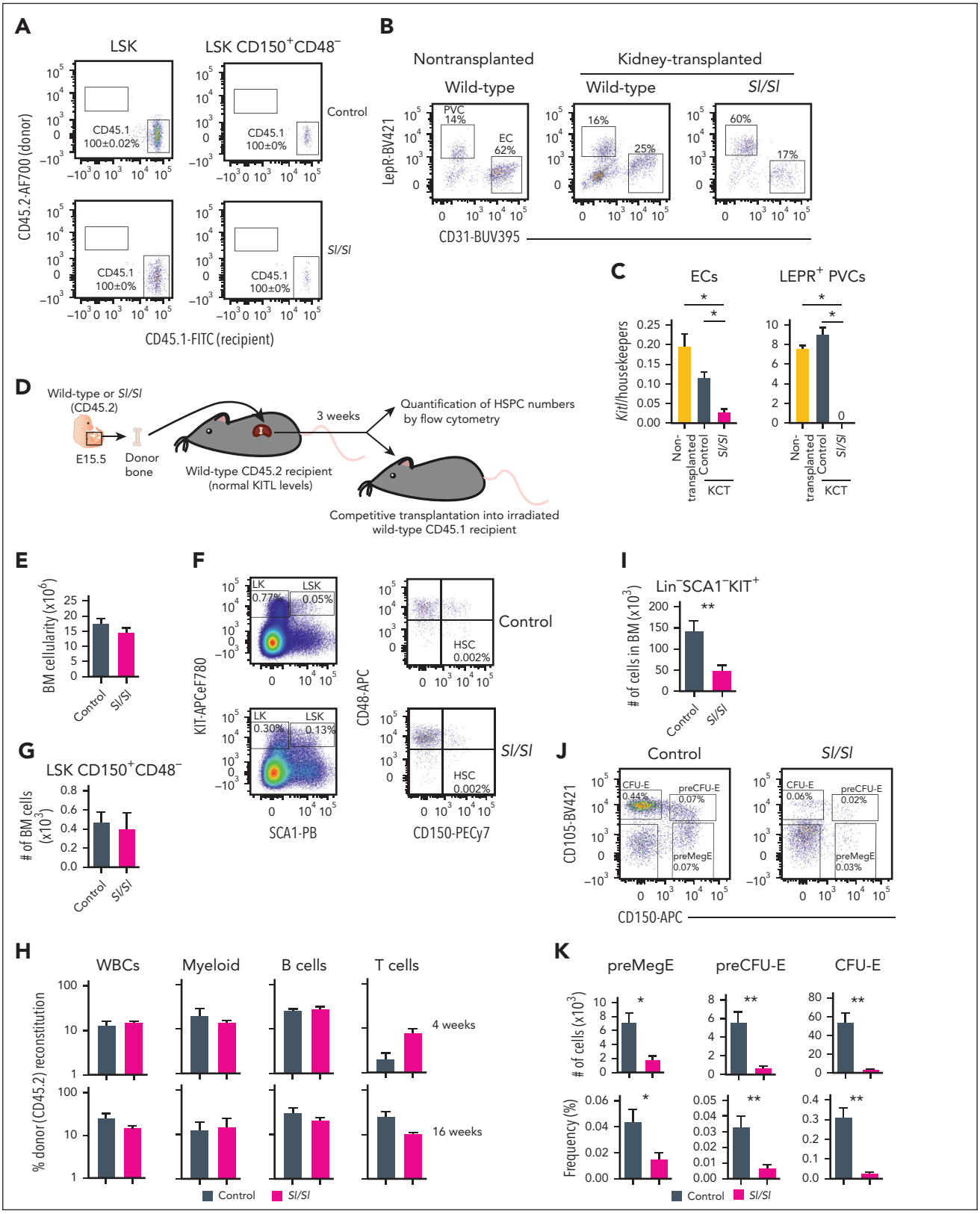

Figure 4. Evidence for a critical role of local BM KITL production for erythropoiesis but not HSCs. (A) Representative FACS profiles and mean (± SEM) percentage recipient CD45.1 reconstitution of LSK and LSK CD150$^+$CD48$^-$ (HSCs) in kidney capsule–transplanted (CD45.2) E15.5 wild-type (control; n = 8) and *Sl/Sl* (n = 4) bones 3 weeks after transplantation. (B) Representative FACS plots showing the distribution of LEPR$^+$ PVCs and CD31$^+$ ECs after first gating as negative for the hematopoietic antigens CD45 and TER119 (CD45$^-$TER119$^-$) in the BM of a nontransplanted femur from 2.5-week-old wild-type mice (n = 5) and in E15.5 femur from wild-type (n = 8) and *Sl/Sl* (n = 4) embryos analyzed 3 to 4 weeks after transplantation under the kidney capsule of wild-type adult recipient mice. (C) Mean (± SEM) expression of total *Kitl* (*Kitl* exon 2-3 amplicon) relative to housekeeping genes (*Hprt*, *B2m*, and *Gapdh*) in ECs and LEPR$^+$ PVCs isolated from femurs of 2.5-week-old wild-type mice (n = 5), and E15.5 femurs from wild-type (n = 5)

Critical role of mKITL in the testis

To determine whether the observed requirement for sKITL, rather than mKITL, for HSCs in the BM might reflect a more general dependence on sKITL rather than mKITL, we investigated whether mKITL might be important for sustaining KIT$^+$ SPCs in the testis,[43] because Sertoli cells that act as niche cells for KIT$^+$ SPCs appear to be highly specific for the testis. In agreement with previous studies, KIT$^+$ SPCs were localized in close proximity to β3-tubulin–positive Sertoli cells in the testis of 4-week-old wild-type mice (Figure 5A). A recent study demonstrated that the combined deletion of sKITL and mKITL in Sertoli cells results in reduced numbers of KIT$^+$ SPCs, but neither the relative role of sKITL and mKITL nor the potential effects on systemic sKITL expression were investigated.[44] We, therefore, specifically ablated mKITL expression in Sertoli cells by generating *Amh-Cre*$^{tg/+}$ (B6.FVB(129S)-Tg(Amh-cre) 8815Reb/J);*Kitl*$^{LEx7/LEx7}$ (AmhΔEx7) mice.[45] Immunostaining with a mKITL specific antibody showed efficient elimination of mKITL in Sertoli cells but not in VE-cadherin–positive ECs from testes of AmhΔEx7 mice (Figure 5B). This was achieved without affecting the systemic levels of sKITL (Figure 5C; supplemental Table 3). Although BM HSC numbers and thymopoiesis were unaffected (supplemental Figure 8A-D), a significant reduction of both KIT$^+$ SPCs and testis size was observed (Figure 5D-E; supplemental Figure 8E-F). Deletion of *Kitl* exon 7 in Sertoli cells was also accompanied by a significant increase in GFRA1$^+$ spermatogonial stem cells that do not express KIT (Figure 5D-E).[46] Therefore, in contrast to HSCs, KIT$^+$ SPCs cannot be sustained by systemic sKITL and require mKITL presented by a specific niche cell type, Sertoli cells, for their maintenance and expansion in the testis.

Discussion

Our findings illuminate the challenges of unraveling the role of specific niche cell types in regulating HSCs residing in BM. In previous studies, specific deletion of *Kitl* (encoding sKITL and mKITL) in ECs resulted in perturbed maintenance of HSCs in BM.[7] This, combined with the observation that *Sld* mutant mice that express sKITL but not mKITL have a severe HSC defect,[5,18,19] led to the conclusion that ECs promote HSC maintenance through the synthesis of KITL in a perivascular HSC niche.[5] However, more recently, we showed that both *Sld* mutant mice and mice with targeted germ line deletion of *mKitl* also have severely reduced systemic levels of sKITL.[21] Not previously investigated, we established here that endothelial-specific deletion of *Kitl*, or only *mKitl*, is also accompanied by significant reductions in systemic sKITL. Despite reduction in the systemic sKITL levels, we failed to observe significantly reduced HSC numbers in the BM of adolescent and adult mice, with complete endothelial deletion of *mKitl*, as well as in adult mice in which *mKitl* was deleted in both ECs and LEPR$^+$ PVCs. In another recent study, the targeted deletion of *mKitl* in ECs in newborn mice was accompanied by a reduction in HSCs, but the effect on systemic sKITL levels was not investigated.[15] Our findings highlight that any finding implicating an EC niche role of mKITL will be limited by the endothelial deletion of *mKitl* also reducing circulating sKITL levels, and by sKITL and mKITL being expressed by ECs elsewhere in the BM as well as in most other tissues and organs.

Our findings fail to support an important HSC regulatory role for mKITL expressed by ECs in BM niches, as previously suggested,[5,7] and are more compatible with BM HSC homeostasis being primarily dependent on the availability of endothelial sKITL, potentially produced by ECs outside HSC niches or even outside the BM. Similar to previous studies, *LepR*^{Cre} was inefficient in reducing *mKitl* expression in LEPR$^+$ PVCs, particularly in adolescent mice, limiting the interpretation of our findings in Tie2,LepRΔEx7 mice failing to support an HSC regulatory role in the BM of mKITL expressed by LEPR$^+$ PVCs. However, and in agreement with previous studies,[36] this was also supported by the lack of an HSC phenotype in *Sl/Sl* (compared with that in wild-type) bones with intact LEPR$^+$ PVCs, with no *Kitl* expression, and ECs, with severely reduced expression, when implanted in wild-type mice with normal circulating sKITL levels. Although these experiments also are compatible with HSC homeostasis in the BM being more dependent on systemic sKITL levels than on local BM expression of either mKITL or sKITL, it is important to emphasize that hematopoiesis in kidney capsule–implanted fetal bones are unlikely to reflect normal steady-state hematopoiesis. In contrast to HSCs, erythroid progenitors, known to also be highly KITL dependent,[42] were reduced in the same kidney capsule–transplanted *Sl/Sl* bones.

How mKITL expression enhances systemic sKITL levels remains unclear. A possible mechanism is through the shedding of mKITL into circulation or binding of mKITL to KIT receptors, enhancing the level of circulating sKITL. Another observation made in our studies was that despite of the significantly reduced systemic levels of sKITL in Tie2ΔEx7 mice, sKITL levels in BM were unaffected, and in Tie2,LeprΔEx7 mice, these levels were even above normal levels. Although the identity and location (within HSC niches or elsewhere inside or outside the BM) of the cells responsible for this compensatory correction of sKITL levels in BM remain to be established, this study further supports a role of sKITL to reduce the impact of reduced sKITL levels in the circulation and/or local mKITL expression on HSC numbers in BM.

Although it is important to emphasize that our findings do not rule out an HSC niche role of endothelial expression of either sKITL or mKITL, they demonstrate that previous genetic models and data fall short of providing strong evidence for the proposed HSC regulatory role of KITL specifically synthesized by

Figure 4 (continued) and *Sl/Sl* (n = 4) embryos 3 to 4 weeks after kidney capsule transplantation (KCT). (D) Experimental design for evaluating impact on hematopoietic stem and progenitor cell (HSPC) numbers within E15.5 wild-type or *Sl/Sl* (*Kitl*-deficient) bones transplanted into recipients with normal levels of KITL. (E) Mean (± SEM) BM cellularity of E15.5 femurs derived from CD45.2 wild-type (control) and *Sl/Sl* mice 3 weeks after transplantation under the kidney capsule of adult CD45.2 wild-type mice (n = 8 of each genotype). (F-G) Representative FACS profiles with gated cell populations as percentages of total BM cells (F) and mean (± SEM) LSK CD150$^+$CD48$^-$ (HSC) numbers (G) per femur (n = 5 of each genotype). (H) Mean (± SEM) PB reconstitution 4 and 16 weeks after competitive transplantation of whole BM cells (CD45.2) from transplanted femurs from (E-G) in competition with wild-type CD45.1 BM cells into irradiated CD45.1 recipients. (I) Mean (± SEM) number of Lin$^-$SCA1$^-$KIT$^+$ (LK) cells (including all committed progenitor cells) in transplanted femurs from panels D and E (n = 8 of each genotype). (J-K) Representative FACS profiles (J) and mean (± SEM) numbers (K, top row) and frequency (K, bottom) of distinct erythroid progenitor subsets in the BM of transplanted femurs from panels D and E (n = 8). All data represent mean ± SEM, and the nonparametric Mann-Whitney test was used to assess statistical significance. *$P < .05$; **$P < .01$.

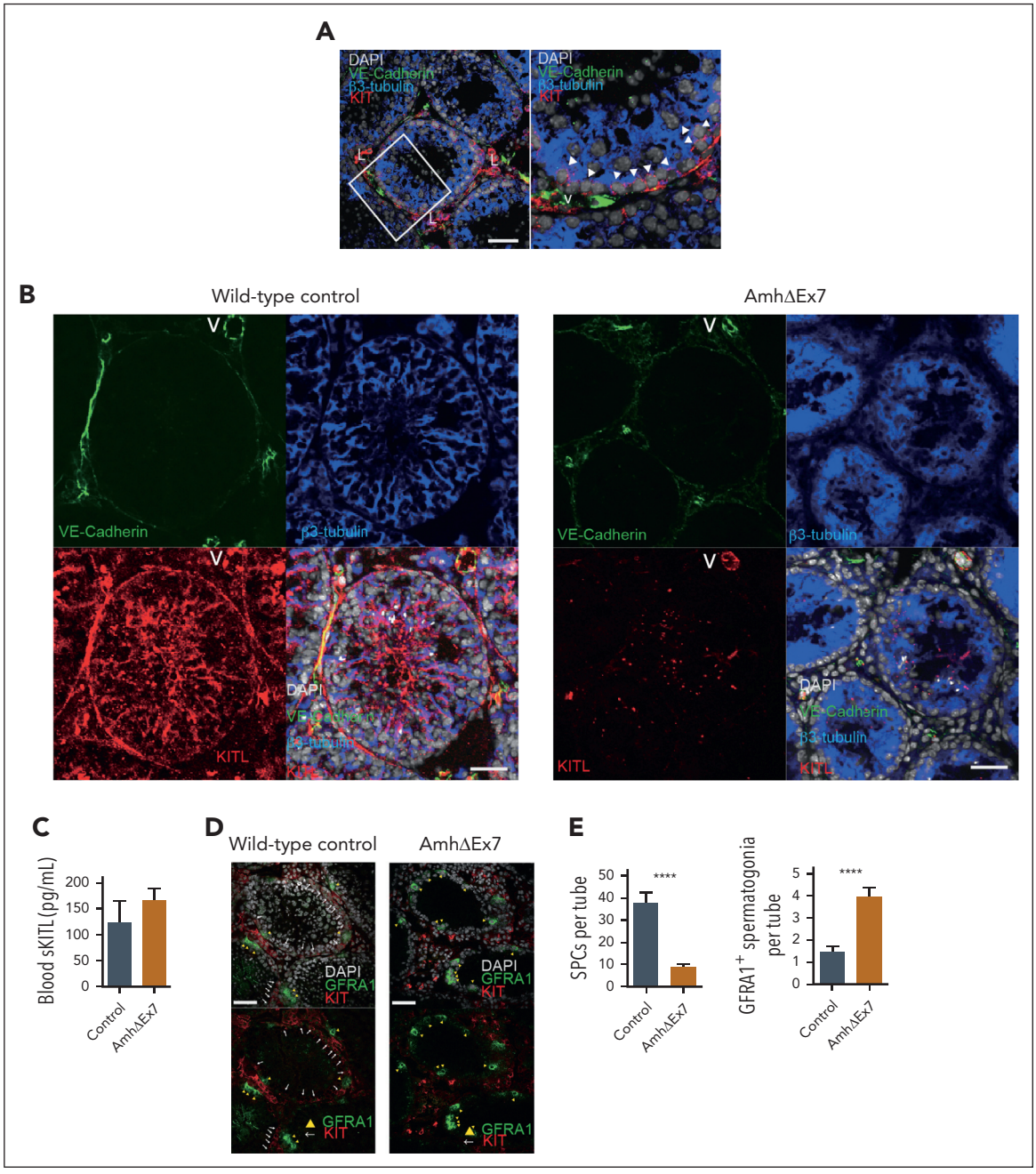

Figure 5. mKITL expression in Sertoli cells is critical for maintenance of Kit$^+$ SPCs in testis. (A) Immunostaining for KIT (red), VE-cadherin (endothelium; green), β3-tubulin (Sertoli cells; blue), counterstained with 4′,6-diamidino-2-phenylindole (DAPI) (nuclear stain; gray) in 4-week-old wild-type mouse testes. Representative of 12 sections from 3 separate mice. Arrow heads: KIT$^+$ spermatogonial precursors adjacent to β3-tubulin$^+$ Sertoli cells. Scale bar represents 50μm. (B) Immunostaining against cytoplasmic domain of mKITL (red), VE-cadherin (green), β3-tubulin (blue), counterstained with DAPI (gray) in 4-week-old AmhΔEx7 and wild-type mouse testes. Representative of 4 to 7 mice of each genotype. Scale bars represent 50μm. (C) Mean (± SEM) blood serum sKITL levels in 4-week old wild-type (control; n = 3) and AmhΔEx7 (n = 7) mice. (D) Immunostaining for KIT (red) and GFRA1 (green), counterstained with DAPI (gray) in 4-week-old wild-type control and AmhΔEx7 mouse testes. White arrows: KIT$^+$ SPCs; yellow arrowhead: GFRA1$^+$ spermatogonia. Representative of 15 mice of each genotype. Scale bars represent 50 μm. (E) Mean (± SEM) KIT$^+$ SPCs and GFRA1$^+$ cells per seminiferous tubule in 4-week-old wild-type (control; n = 19) and AmhΔEx7 (n = 30) testes (mean ± SEM). More than or equal to 50 round cross sections of seminiferous tubules were counted per genotype. The nonparametric Mann-Whitney test for multiple comparisons was used to assess statistical significance. ****P < .0001. L, KIT$^+$ Leydig cells; V, blood vessel.

ECs in perivascular BM niches for HSCs.[5,7] Most importantly, our studies highlight the hurdles that must be overcome to establish in a more definitive manner the regulatory roles of specific HSC niche cells and extrinsic cues in the BM. To date, to our knowledge, no proposed candidate HSC niche cells or regulators have been convincingly shown to be unique to the proposed anatomical HSC niches or BM, nor have any tools been developed to genetically modify candidate niche cells in a niche-specific or even BM-specific manner. Herein, the specific depletion of mKITL in Sertoli cells in the testis, reproducing the KIT$^+$ sperm cell precursor deficiency of KITL-deficient mice,[43] without affecting circulating sKITL levels, illustrates how a

highly specific deletion of mKITL expression in a niche cell population (specific to the testis) can establish the identity of a distinct niche cell and its role in the local regulation of a distinct stem/progenitor cell, through mKITL expression in this case. A similar niche role for mKITL has also been suggested for KIT$^+$ thymic progenitors.[21] Although the tightly regulated number of HSCs and other findings are consistent with the importance of distinct BM HSC niches, more unequivocal insights into the identity and functional roles of such niches await application of more specific genetic approaches.

Acknowledgments

The authors thank Sean Morrison for sharing the Kitl$^{tm2.1Sjm}$/J mice and for critical input on these studies, Peter Besmer for providing the antibody against the intracellular region of KITL, the Medical Research Council Weatherall Institute of Molecular Medicine (MRC WIMM) Flow Cytometry core facility for assistance with fluorescence-activated cell sorting (supported by the MRC Human Immunology Unit, MRC Molecular Haematology Unit [MC_UU_12009], The National Institute for Health and Care Research Oxford BRC, and the John Fell Fund [131/030 and 101/517]), and the University of Oxford Biomedical Services for assistance with managing the mouse strains.

This work was supported by the MRC United Kingdom (G0801073 and MC_UU_12009/5 [S.E.W.J.] and MC_UU_12009/7 [C.N.]), Kay Kendall Leukaemia Fund (S.E.W.J. and T.C.L.), the Swedish Research Council (538-2013-8995 [S.E.W.J.] and 2015-03561 [P.S.W.]), the Knut och Alice Wallenberg Foundation (KAW 2016.0105 [S.E.W.J.] and KAW 2015.0195 [P.S.W.]), StratRegen KI (S.E.W.J.), and Wellcome Trust Sir Henry Dale Fellowship (T.C.L.) (210424/Z/18/Z).

Authorship

Contribution: S.E.W.J. and C.N. conceptualized the project; S.M., R.F., T.C.L., J.C., P.S.W., F.A., T.S., A.J.M., C.N., and S.E.W.J. designed the experiments; S.M., R.F., T.C.L., T.M., J.C., H.B., M.B., R.N., and B.W. performed the experiments; S.M., R.F., T.C.L., P.S.W., C.N., and S.E.W.J. wrote the manuscript; and all authors analyzed the experiments, examined and had the opportunity to edit the manuscript, and approved the final manuscript.

Conflict-of-interest disclosure: The authors declare no competing financial interests.

ORCID profiles: R.F., 0000-0002-6026-6893; T.C.L., 0000-0002-6305-1257; J.C., 0000-0002-0324-2617; P.S.W., 0000-0002-2340-2526; S.E.W.J., 0000-0002-1362-3659.

Correspondence: Sten Eirik W. Jacobsen, Department of Medicine Huddinge, Hematopoietic Stem Cell Laboratory, Center for Hematology and Regenerative Medicine, Box 285, 17177 Stockholm, Sweden; email: sten.eirik.jacobsen@ki.se; and Claus Nerlov, Stem Cell Biology, Medical Research Council Molecular Haematology Unit at the University of Oxford, MRC Weatherall Institute of Molecular Medicine, John Radcliffe Hospital, Headington, Oxford OX3 9DS, United Kingdom; email: claus.nerlov@imm.ox.ac.uk.

Footnotes

Submitted 10 November 2022; accepted 25 July 2023; prepublished online on *Blood* First Edition 10 August 2023. https://doi.org/10.1182/blood.2022019018.

*S.M., R.F., T.C.L., J.C., and P.S.W. contributed equally to the work.

†C.N. and S.E.W.J. contributed equally to the work.

All data are available within manuscript or on request from the corresponding author, Sten Eirik W. Jacobsen (sten.eirik.jacobsen@ki.se).

The online version of this article contains a data supplement.

There is a *Blood* Commentary on this article in this issue.

The publication costs of this article were defrayed in part by page charge payment. Therefore, and solely to indicate this fact, this article is hereby marked "advertisement" in accordance with 18 USC section 1734.

REFERENCES

1. Zon LI. Intrinsic and extrinsic control of haematopoietic stem-cell self-renewal. *Nature*. 2008;453(7193):306-313.
2. Schofield R. The relationship between the spleen colony-forming cell and the haemopoietic stem cell. *Blood Cells*. 1978;4(1-2):7-25.
3. Pinho S, Frenette PS. Haematopoietic stem cell activity and interactions with the niche. *Nat Rev Mol Cell Biol*. 2019;20(5):303-320.
4. Crane GM, Jeffery E, Morrison SJ. Adult haematopoietic stem cell niches. *Nat Rev Immunol*. 2017;17(9):573-590.
5. Morrison SJ, Scadden DT. The bone marrow niche for haematopoietic stem cells. *Nature*. 2014;505(7483):327-334.
6. Calvi LM, Adams GB, Weibrecht KW, et al. Osteoblastic cells regulate the haematopoietic stem cell niche. *Nature*. 2003;425(6960):841-846.
7. Ding L, Saunders TL, Enikolopov G, Morrison SJ. Endothelial and perivascular cells maintain haematopoietic stem cells. *Nature*. 2012;481(7382):457-462.
8. Zhao M, Perry JM, Marshall H, et al. Megakaryocytes maintain homeostatic quiescence and promote post-injury regeneration of hematopoietic stem cells. *Nat Med*. 2014;20(11):1321-1326.
9. Yamazaki S, Ema H, Karlsson G, et al. Nonmyelinating Schwann cells maintain hematopoietic stem cell hibernation in the bone marrow niche. *Cell*. 2011;147(5):1146-1158.
10. Mendez-Ferrer S, Michurina TV, Ferraro F, et al. Mesenchymal and haematopoietic stem cells form a unique bone marrow niche. *Nature*. 2010;466(7308):829-834.
11. Kunisaki Y, Bruns I, Scheiermann C, et al. Arteriolar niches maintain haematopoietic stem cell quiescence. *Nature*. 2013;502(7473):637-643.
12. Christodoulou C, Spencer JA, Yeh SCA, et al. Live-animal imaging of native haematopoietic stem and progenitor cells. *Nature*. 2020;578(7794):278-283.
13. Broudy VC. Stem cell factor and hematopoiesis. *Blood*. 1997;90(4):1345-1364.
14. Huang E, Nocka K, Beier DR, et al. The hematopoietic growth factor KL is encoded by the Sl locus and is the ligand of the c-kit receptor, the gene product of the W locus. *Cell*. 1990;63(1):225-233.
15. Kara N, Xue Y, Zhao Z, et al. Endothelial and leptin receptor(+) cells promote the maintenance of stem cells and hematopoiesis in early postnatal murine bone marrow. *Dev Cell*. 2023;58(5):348-360.e6.
16. Flanagan JG, Chan DC, Leder P. Transmembrane form of the kit ligand growth factor is determined by alternative splicing and is missing in the Sld mutant. *Cell*. 1991;64(5):1025-1035.
17. Zhou BO, Yue R, Murphy MM, Peyer JG, Morrison SJ. Leptin-receptor-expressing mesenchymal stromal cells represent the main source of bone formed by adult bone marrow. *Cell Stem Cell*. 2014;15(2):154-168.
18. Barker JE. Sl/Sld hematopoietic progenitors are deficient in situ. *Exp Hematol*. 1994;22(2):174-177.
19. Barker JE. Early transplantation to a normal microenvironment prevents the development of Steel hematopoietic stem cell defects. *Exp Hematol*. 1997;25(6):542-547.
20. Wolf NS. Dissecting the hematopoietic microenvironment. III. Evidence for a positive short range stimulus for cellular proliferation. *Cell Tissue Kinet*. 1978;11(4):335-345.
21. Buono M, Facchini R, Matsuoka S, et al. A dynamic niche provides Kit ligand in a

stage-specific manner to the earliest thymocyte progenitors. *Nat Cell Biol*. 2016;18(2):157-167.

22. He L, Vanlandewijck M, Mae MA, et al. Single-cell RNA sequencing of mouse brain and lung vascular and vessel-associated cell types. *Sci Data*. 2018;5:180160.

23. Vanlandewijck M, He L, Mae MA, et al. A molecular atlas of cell types and zonation in the brain vasculature. *Nature*. 2018;554(7693):475-480.

24. Foster BM, Langsten KL, Mansour A, Shi L, Kerr BA. Tissue distribution of stem cell factor in adults. *Exp Mol Pathol*. 2021;122:104678.

25. Schwenk F, Baron U, Rajewsky K. A cre-transgenic mouse strain for the ubiquitous deletion of loxP-flanked gene segments including deletion in germ cells. *Nucleic Acids Res*. 1995;23(24):5080-5081.

26. DeFalco J, Tomishima M, Liu H, et al. Virus-assisted mapping of neural inputs to a feeding center in the hypothalamus. *Science*. 2001;291(5513):2608-2613.

27. Holdcraft RW, Braun RE. Androgen receptor function is required in Sertoli cells for the terminal differentiation of haploid spermatids. *Development*. 2004;131(2):459-467.

28. Comazzetto S, Murphy MM, Berto S, Jeffery E, Zhao Z, Morrison SJ. Restricted hematopoietic progenitors and erythropoiesis require SCF from leptin receptor+ niche cells in the bone marrow. *Cell Stem Cell*. 2019;24(3):477-486.e6.

29. Sarvella PA, Russell LB. Steel, a new dominant gene in the house mouse. *J Hered*. 1956;47(3):123-128.

30. Sato T, Yokonishi T, Komeya M, et al. Testis tissue explantation cures spermatogenic failure in c-Kit ligand mutant mice. *Proc Natl Acad Sci U S A*. 2012;109(42):16934-16938.

31. Sanjuan-Pla A, Macaulay IC, Jensen CT, et al. Platelet-biased stem cells reside at the apex of the haematopoietic stem-cell hierarchy. *Nature*. 2013;502(7470):232-236.

32. Pronk C, Rossi D, Månsson R, et al. Elucidation of the phenotypic, functional, and molecular topography of a myeloerythroid progenitor cell hierarchy. *Cell Stem Cell*. 2007;1(4):428-442.

33. Moreau JM, Berger A, Nelles ME, et al. Inflammation rapidly reorganizes mouse bone marrow B cells and their environment in conjunction with early IgM responses. *Blood*. 2015;126(10):1184-1192.

34. Luis TC, Luc S, Mizukami T, et al. Initial seeding of the embryonic thymus by immune-restricted lympho-myeloid progenitors. *Nat Immunol*. 2016;17(12):1424-1435.

35. Wilkinson AC, Igarashi KJ, Nakauchi H. Haematopoietic stem cell self-renewal in vivo and ex vivo. *Nat Rev Genet*. 2020;21(9):541-554.

36. Chan CK, Chen CC, Luppen CA, et al. Endochondral ossification is required for haematopoietic stem-cell niche formation. *Nature*. 2009;457(7228):490-494.

37. Varas F, Grande T, Ramirez A, Bueren JA. Implantation of bone marrow beneath the kidney capsule results in transfer not only of functional stroma but also of hematopoietic repopulating cells. *Blood*. 2000;96(6):2307-2309.

38. Motro B, van der Kooy D, Rossant J, Reith A, Bernstein A. Contiguous patterns of c-kit and steel expression: analysis of mutations at the W and Sl loci. *Development*. 1991;113(4):1207-1221.

39. Christensen JL, Wright DE, Wagers AJ, Weissman IL. Circulation and chemotaxis of fetal hematopoietic stem cells. *PLoS Biol*. 2004;2(3):E75.

40. Coşkun S, Chao H, Vasavada H, et al. Development of the fetal bone marrow niche and regulation of HSC quiescence and homing ability by emerging osteolineage cells. *Cell Rep*. 2014;9(2):581-590.

41. Hall TD, Kim H, Dabbah M, et al. Murine fetal bone marrow does not support functional hematopoietic stem and progenitor cells until birth. *Nat Commun*. 2022;13(1):5403.

42. Russell ES. Hereditary anemias of the mouse: a review for geneticists. *Adv Genet*. 1979;20:357-459.

43. Rossi P, Sette C, Dolci S, Geremia R. Role of c-kit in mammalian spermatogenesis. *J Endocrinol Invest*. 2000;23(9):609-615.

44. Peng YJ, Tang XT, Shu HS, Dong W, Shao H, Zhou BO. Sertoli cells are the source of stem cell factor for spermatogenesis. *Development*. 2023;150(6):dev200706.

45. Lecureuil C, Fontaine I, Crepieux P, Guillou F. Sertoli and granulosa cell-specific Cre recombinase activity in transgenic mice. *Genesis*. 2002;33(3):114-118.

46. Nakagawa T, Sharma M, Nabeshima Y, Braun RE, Yoshida S. Functional hierarchy and reversibility within the murine spermatogenic stem cell compartment. *Science*. 2010;328(5974):62-67.